DRAFT CONF-820833--10 Draft

Carbon-14 Immobilization via the $Ba(OH)_2 \cdot 8H_2O$ Process*

G. L. Haag
J. W. Nehls, Jr.
G. C. Young

Chemical Technology Division
Oak Ridge National Laboratory
Oak Ridge, Tennessee 37830

CONF-820833--10 DRAFT

DE82 020834

For presentation at the 17th DOE Nuclear Air Cleaning Conference, Denver, Colorado, August 2-5, 1982; to be published in the Proceedings.

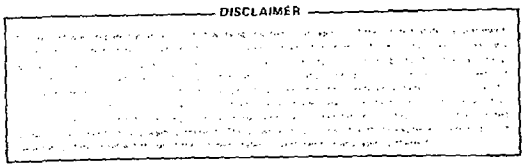

*Research sponsored by the Division of Waste Products, Office of Nuclear Waste Management, U.S. Department of Energy under contract W-7405-eng-26 with the Union Carbide Corporation.

CARBON-14 IMMOBILIZATION VIA THE $Ba(OH)_2 \cdot 8H_2O$ PROCESS*

G. L. Haag, J. W. Nehls, Jr., and G. C. Young
Chemical Technology Division
Oak Ridge National Laboratory
Oak Ridge, Tennessee

Abstract

The airborne release of ^{14}C from various nuclear facilities has been identified as a potential biohazard due to the long half-life of ^{14}C (5730 yrs) and the ease in which it may be assimilated into the biosphere. At Oak Ridge National Laboratory, technology is under development, as part of the Airborne Waste Management Program, for the removal and immobilization of this radionuclide. Prior studies have indicated that the ^{14}C will likely exist in the oxidized form as CO_2 and will contribute slightly to the bulk CO_2 concentration of the gas stream, which is airlike in nature (~330 ppm_v CO_2). The technology under development utilizes the $CO_2 - Ba(OH)_2 \cdot 8H_2O$ gas-solid reaction with the mode of gas-solid contacting being a fixed bed. The product, $BaCO_3$, possessing excellent thermal and chemical stability, prerequisites for the long-term disposal of nuclear wastes. For optimal process operation, studies have indicated that an operating window of adequate size does exist. When operating within the window, high CO_2 removal efficiency (effluent concentrations <100 ppb_v), high reactant utilization (>99%), and an acceptable pressure drop across the bed (3 kPa/m at 13 cm/s superficial velocity) are possible. This paper will address three areas of experimental investigation. These areas are (1) micro-scale studies on 150-mg samples to provide information concerning surface properties, kinetics, and equilibrium vapor pressures, (2) macro-scale studies on large fixed beds (4.2 kg reactant) to determine the effects of humidity, temperature, and gas flow-rate upon bed pressure drop and CO_2 breakthrough, and (3) the design, construction, and initial operation of a pilot unit capable of continuously processing a 34 m^3/h (20 ft^3/min) air-based gas stream.

*Research sponsored by the Division of Waste Products, Office of Nuclear Waste Management, U.S. Department of Energy under contract W-7405-eng-26 with the Union Carbide Corporation.

I. Introduction

The release of ^{14}C from the nuclear fuel cycle has been identified as a potential biohazard because of its long half-life of 5730 years and the ease in which it may be assimilated into the biosphere.[1-20] In nuclear reactors, ^{14}C is produced primarily by neutron interactions with ^{13}C, ^{14}N, and ^{17}O which are present in the fuel, the cladding, and the coolant. The bulk of the ^{14}C is released in the gaseous form at either the reactor or upon reprocessing of the spent fuel. Presented in Table I are representative release rates at various nuclear facilities.

Table I. Approximate production and release rates[2]

Nuclear reactors	Ci/Gw(e)yr
LWR	8-10
CANDU	500
Reprocessing plant	
LMFBR	6
LWR	18
HTGR	200

^{14}C, like ^{3}H, ^{85}Kr, ^{129}I, is a global radionuclide. That is, upon release to the environment, its dosage impact is not limited to the region of release, a release which may be legislated by local government, but rather the net dosage is distributed globally in a nearly uniform manner. Furthermore because of its long half-life, ^{14}C release poses a health hazard to both present and future generations. Modeling studies have been conducted for predicting the dosage effects from ^{14}C release. However, these studies require major assumptions concerning the effects of low-level radiation, future population growth, and the time period of dosage integration. Depending upon the assumptions, total dosage estimates typically

vary from 400 to 590 man-rem/curie. In a modeling study by Killough and Rohwer at ORNL, a total dosage estimate of 540 man-rem/curie was obtained. This study also predicted dosage estimates for time periods of 30 and 100 years of 18 and 23 man-rem/curie, respectively.[17] More recent modeling studies by Killough et. al. have indicated that for ^{14}C release from a 30.5 m (100-ft) stack at the Morris, Ill. or Barnwell, S. C. reprocessing plants, .02 and .002% of the total dosage would occur within 100 km of the respective points of release.[18] A study by the Nuclear Energy Agency (NEA) on the release of global radionuclides ^{3}H, ^{14}C, ^{85}Kr, and ^{129}I restricted the time period of interest to 10,000 years. Hence a partial dosage for ^{14}C of 290 man-rem/curie was used.[16] With knowledge of the worldwide release of ^{14}C, the resulting dosage per curie released, and assuming 146 fatal health effects, 105 nonfatal cancers, and 76 serious genetic effects per million man-rem of dosage as estimated by Fowler and Nelson,[20] an estimate of the health effects resulting from ^{14}C release may be made. However these health effects must be placed in the proper perspective. That is they may occur anyplace and anytime within the time limits of dosage integration. For global radionuclides with long half-lives such as ^{14}C, the often cited cost effective values of $100 to $1000 per man-rem for controlling radionuclide release may not be justified, as certain questions of a philosophical and technical nature must first be answered. However if a technology of suitable cost-effectiveness is shown to exist, the control of ^{14}C release will then be warranted. Therefore, the primary goal of this research effort is to develop such a cost-effective technology.

II. Technology Development

In the development of technology for controlling the release of ^{14}C from the nuclear fuel cycle, we have established the following criteria for candidate processes:

A. An acceptable process efficiency, nominal decontamination factor of 10.

B. An acceptable final product form for long-term waste disposal.

C. Excellent on-line process characteristics.

D. Process operation at near-ambient conditions.

E. Acceptable process costs (<$10/man-rem).

Based upon these criteria, an operationally simple process which utilizes fixed-bed cannisters of $Ba(OH)_2 \cdot 8H_2O$ has been developed at ORNL. At ambient temperatures and pressures, this process is capable of removing CO_2 (330 ppm_v) in air to concentrations <100 ppb_v. Thermodynamic calculations indicate equilibrium concentrations to be at the part per trillion level.[21] The product, $BaCO_3$, possesses excellent thermal and chemical stability as it decomposes at 1450°C and is sparingly soluble in water, 0.124 mg-mol/L at 25°C.[22,23] Furthermore, the soluble reactant reacts to 100% conversion thus insuring an extremely stable material for final disposal. Gas throughputs are such that reactor size remains practical for the treatment of anticipated process streams. For a design superficial velocity of 13 cm/s, a reactor with a diameter of 0.70 m (27 in.) would be required for the treatment of a 170 m^3/h (100 ft^3/min) off-gas stream. Although extensive cost studies have not been completed, initial comparative studies with alternatives technologies have indicated the process to be extremely cost competitive.[16,20,24-31] The estimated process cost is <$10/man-rem.

The intent of this paper will be to highlight the contents of two major technical reports that are in preparation.[32,33] For additional information, these reports should be consulted. Studies concerning the development of the $Ba(OH)_2 \cdot 8H_2O$ process for $^{14}CO_2$ removal will be broken into 3 areas: (1) micro-scale studies, (2) fixed-bed macro-scale studies, and (3) the design and operation of a pilot plant.

Experimental studies have concentrated upon the use of flakes of $Ba(OH)_2 \cdot 8H_2O$. As shown in Fig. 1, the material is a free-flowing solid and when reacted with CO_2 under the proper conditions, the flake-form remains intact upon conversion to $BaCO_3$. Vendor specifications indicate the material to be substoichiometric in water and to possess an overall hydration of 7.0 to 7.9 H_2O. Discussions with the vendor

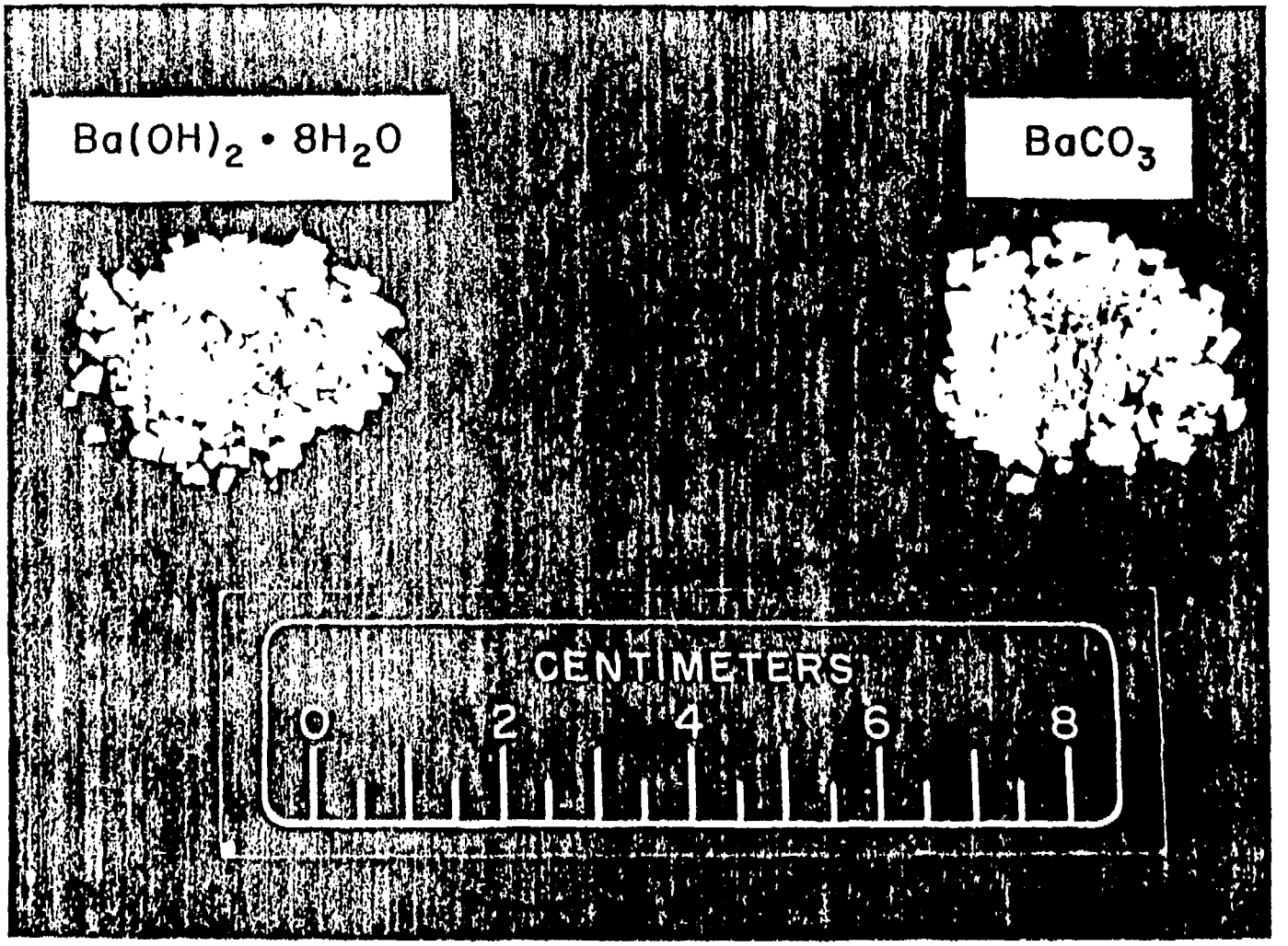
$Ba(OH)_2 \cdot 8H_2O$
$BaCO_3$
CENTIMETERS
0
2
4
6
8

indicated the water deficiency to be intentional so as to insure a free-flowing non-sticking product.

The flakes are prepared by the distribution of a $Ba(OH)_2$ hydrate magma (~78°C) on a stainless steel conveyor belt, which is cooled on the underside with cooling water.[34] The resulting flakes are variable in thickness, an average thickness of 0.10 cm (1/16 in.). Presented in Table II are the results of a particle-size analysis on material originating from different batch numbers. Analysis of samples

Table II. Particle size analysis of commercial $Ba(OH)\cdot 8H_2O$ flakes obtained from two different batch numbers

Particle size		Weight %	
Mesh	mm	Batch #1	Batch #2
4 +	4.75	18.5	5.8
8 + 4	2.36 + 4.75	46.9	33.0
20 + 8	.850 + 236	31.6	54.5
50 + 20	.300 + .850	2.0	4.9
120 +	.125 + .300	.4	1.2
+ 120	+ .125	.6	.6

obtained from the two batches indicated stoichiometries of approximately 7.5 and 7.0 H_2O, respectively. For a given batch number, little variation was observed in the extent of hydration. X-ray analysis of the two samples failed to confirm the presence of $Ba(OH)_2\cdot 3H_2O$, the next stable hydrate of lower stoichiometry. However, the existence of a $Ba(OH)_2\cdot 3H_2O$–$Ba(OH)_2\cdot 8H_2O$ eutectic with an overall water stoichiometry of 7.19 has been reported.[35,36] It is speculated that the failure to detect the trihydrate species results from an extremely small crystallite size. Sorption isotherm studies indicated the reactant to display negligible microporosity ($d < 2$ nm) or restrictive mesoporosity (2 nm $< d <$ 150 nm). Mercury porosimetry studies indicated the pore size distribution to be bimodal with maximas of 0.17 and 1.0 μm and a flake porosity of 12%. It was observed that when a flake was exposed to a water

vapor pressure that was < or > the vapor pressure of $Ba(OH)_2 \cdot 8H_2O$, the material either dehydrated to the trihydrate or hydrated to the octahydrate. Rehydration was observed to proceed in one of two regimes and to be dependent upon the relative humidity. This factor will be addressed in subsequent sections. The best correlation for predicting the vapor pressure of $Ba(OH)_2 \cdot 8H_2O$ appears to be that presented by Kondakov et.al.[37]

$$\text{Log}(P) = -\frac{58230}{19.155T} + 13.238$$

where

P = pressure, Pa or nt/m^2, and

T = temperature, K.

With respect to published vapor pressure data on $Ba(OH)_2 \cdot 8H_2O$, a comprehensive, chronological review of the published vapor pressures is presented elsewhere by the authors.[32]

As shown in Fig. 1, operating conditions exist for which the integrity of the flake-form is retained upon conversion to $BaCO_3$. Because of the low molar volume of the product as compared to that of the reactant, a ratio of 0.31, and an initial particle voidage of 12%, one would predict a final product porosity of 73%. Mercury porosimetry studies have indicated product porosities of 66 to 72%.[21,32] Visual evidence of this porosity may be observed by comparing scanning electron micrographs of the reactant and product (Fig. 2).

With respect to $Ba(OH)_2$ hydrate nomenclature, the following convention will be used in the remainder of this paper. The substoichiometric flakes will be referred to as commercial $Ba(OH)_2 \cdot 8H_2O$ (7.5). Where it is of significance, the term in parenthesis will refer to the initial hydration stoichiometry. The term $Ba(OH)_2 \cdot 8H_2O$ will refer to the stable crystalline species with 8 waters of hydration.

III. Micro-Scale Studies

Realizing that an understanding or at least an awareness of phenomenon which occur on the micro-scale is often required to develop an understanding of macro-scale

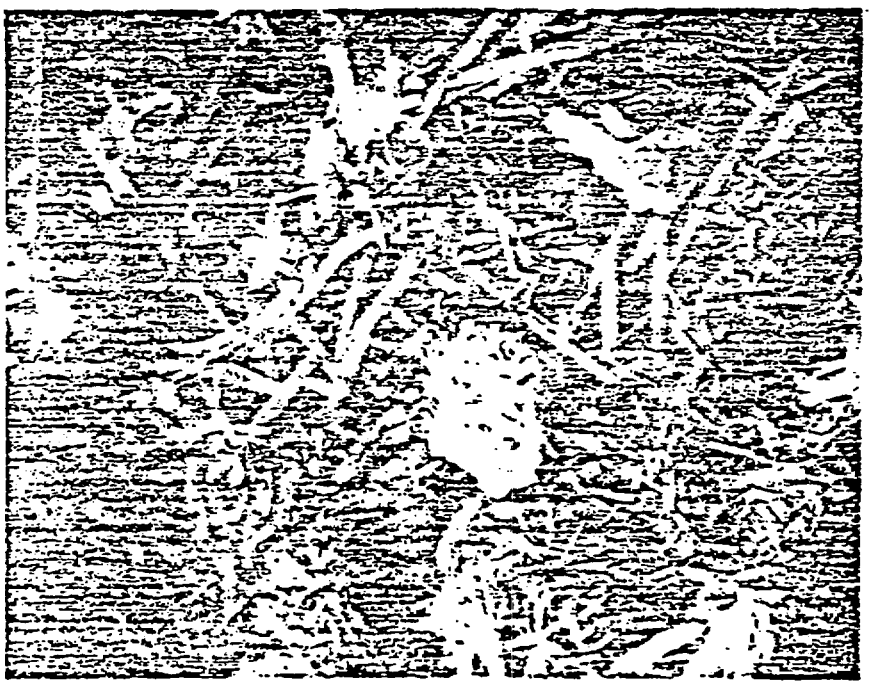

Fig 2

phenomenon, basic studies were conducted on the hydrates of $Ba(OH)_2$ and the $BaCO_3$ product. Analytical techniques consisted of scanning electron microscopy, mercury intrusion for porosimetry determination, acid-base titrations and overall mass balances to determine the extent of conversion and hydration, x-ray diffraction analysis, single-point BET analysis, and the operation of a microbalance system whereby studies of a kinetic, thermodynamic, and surface morphological nature could be performed on 150 mg samples (Fig. 3). Results from these studies were useful in the characterization of the $Ba(OH)_2 \cdot 8H_2O$ reactant which was reported in the preceeding section. The intent of this section will be to highlight experimental results from these studies. Detailed information will be available in a previously cited report that is in preparation.[32] Highlights from the micro-scale studies are:

A. Methods of preparation of $Ba(OH)_2 \cdot H_2O$, $Ba(OH)_2 \cdot 3H_2O$ and $Ba(OH)_2 \cdot 8H_2O$ were developed and the presence of said species confirmed.

B. Commercial $Ba(OH)_2 \cdot 8H_2O$ flakes were found to display negligible surface area. Hydration to $Ba(OH)_2 \cdot 8H_2O$ was observed to proceed in one of two regimes. For relative humidities <60%, the increase in surface area was small and the flake-form remained intact. For relative humidities >60%, the flake recrystallized in a manner which resulted in greater surface area, but the increase in activity also resulted in a more fragile product.

C. Dehydration of commercial $Ba(OH)_2 \cdot 8H_2O$ to $Ba(OH)_2 \cdot 3H_2O$ and subsequent rehydration to $Ba(OH)_2 \cdot 8H_2O$ at relative humidities <60% was modeled by a shrinking core model. The relative rate was found to be dependent upon the difference between the water sorbed on the surface for a given P/P_o value (i.e. relative humidity) and that required on the surface for $Ba(OH)_2 \cdot 8H_2O$ to exist in a stable form.

D. There was evidence of considerable hydrogen bonding within the $Ba(OH)_2 \cdot 8H_2O$ crystal. These results paralleled the crystallography studies of Monohar and Ramaseshan in which they cited difficulty in differentiating the location of the hydroxyl ions from the waters of hydration.[38]

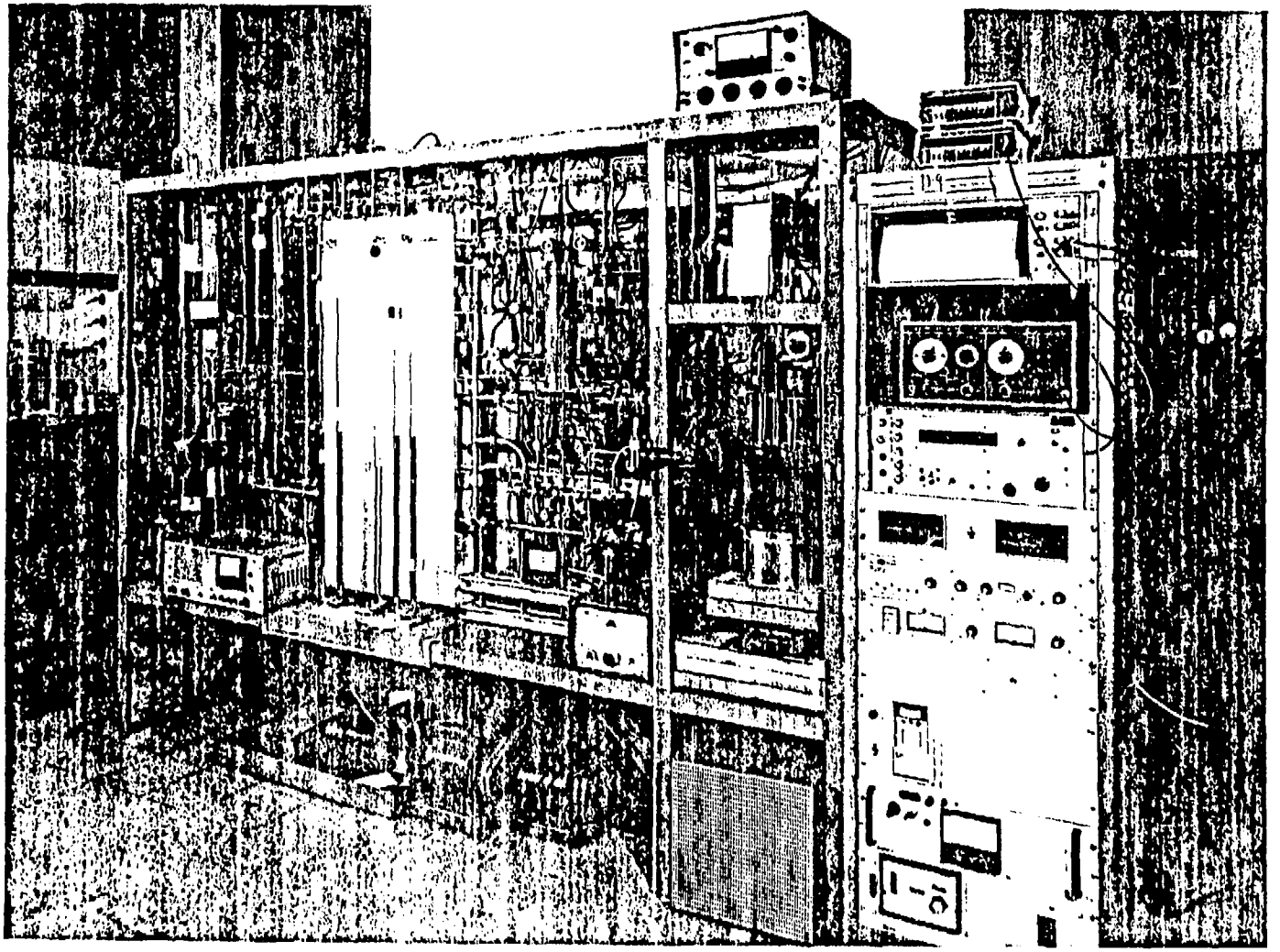

E. The vapor pressure correlation for $Ba(OH)_2 \cdot 8H_2O$ cited in the previous section was indirectly verified at two temperatures.

F. At low CO_2 vapor pressures, $Ba(OH)_2 \cdot 8H_2O$ was observed to be 3 orders of magnitude more reactive toward CO_2 than either $Ba(OH)_2 \cdot 3H_2O$ or $Ba(OH)_2 \cdot H_2O$.

G. For relative humidities <60%, the increase in surface area with product conversion was found to be a very strong function of the specific rate of reaction and was not a linear function of conversion.

H. The surface area of $BaCO_3$ product was determined to be a function of relative humidity. In a manner analogous to the dehydration of commercial $Ba(OH)_2 \cdot 8H_2O$ and the rehydration of $Ba(OH)_2 \cdot 3H_2O$, surface water appears to aid in the transport of the reactant and product species, thus resulting in lower surface areas at higher values of P/P_o (i.e. relative humidity). However, it is the opinion of the authors that the increase in surface water could not account for the drastic difference in CO_2 reactivity observed for the various hydrate species. The difference in reactivity appears to result from the additional water in the crystal structure and the greater mobility of the hydroxyl ions.

I. Based upon the analysis of nitrogen sorption isotherm data, there were no indications of hysteresis. Therefore if capillary condensation should occur, one would speculate it to result from the wall effects of noncircular pores (ex. V-shaped points of intersurface contact).

IV. Fixed-bed macro-scale studies

Over 18,000 hours of experimental operating time have been obtained on fixed-beds of $Ba(OH)_2 \cdot 8H_2O$. These beds typically contained from 2.9 to 4.3 kg of reactant. A schematic of the experimental system, which has been described in detail in a previous paper, is presented in Fig. 4.[21] The intent of this aspect of the study was to determine the effects of air flowrate (superficial gas velocities of 7-21 cm/s), operating temperature (22-42°C), and water vapor pressure or relative humidity (0-80%) upon the operational characteristics of the fixed bed, most notably the shape of the breakthrough curve and the pressure drop across the fixed bed. As the

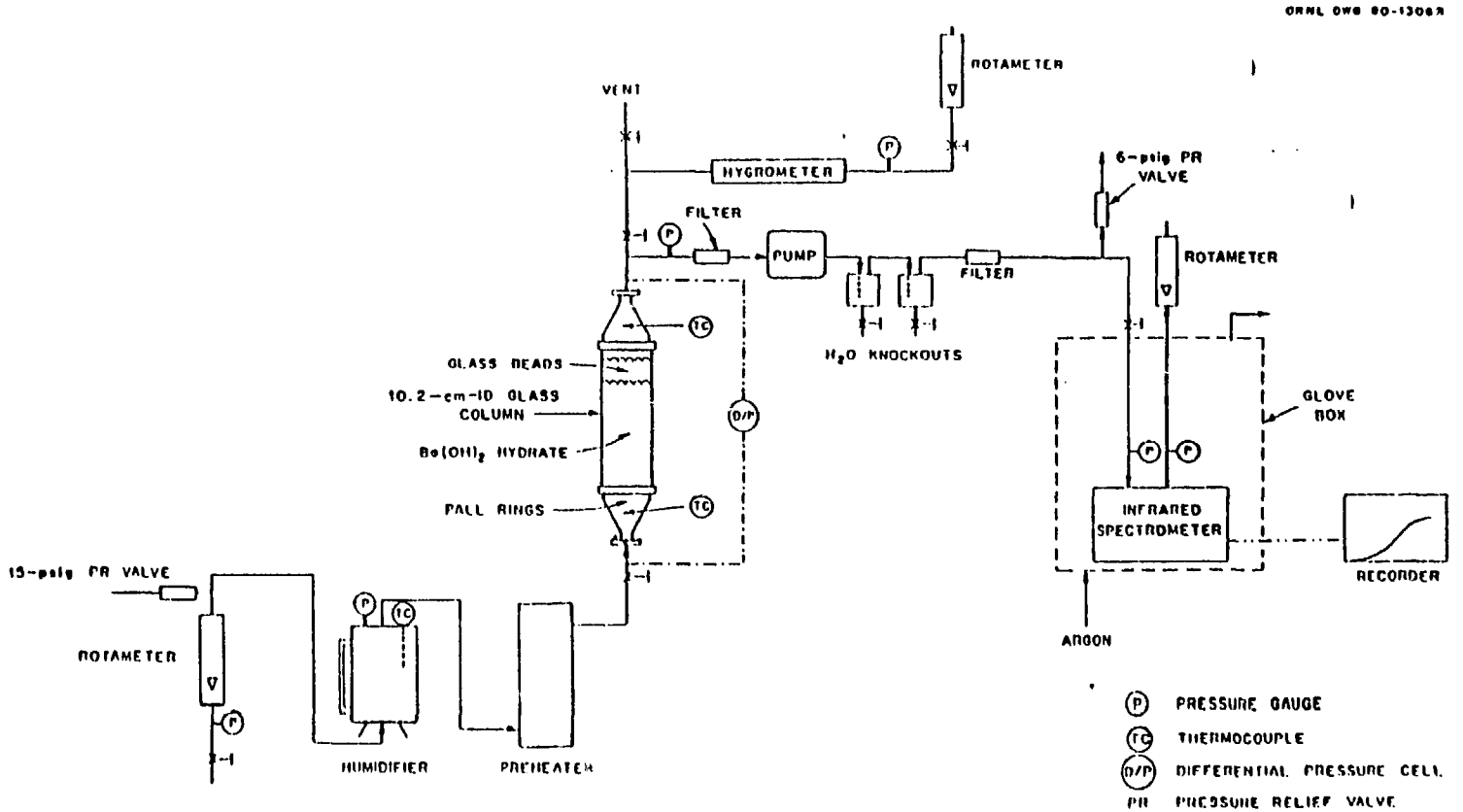
ORNL DWG 80-13068R
ROTAMETER
VENT
HYGROMETER
6-psig PR VALVE
FILTER
PUMP
FILTER
ROTAMETER
GLASS BEADS
10.2-cm-ID GLASS COLUMN
Ba(OH)2 HYDRATE
PALL RINGS
H2O KNOCKOUTS
GLOVE BOX
INFRARED SPECTROMETER
RECORDER
15-psig PR VALVE
ROTAMETER
HUMIDIFIER
PREHEATER
ARGON
PRESSURE GAUGE
THERMOCOUPLE
DIFFERENTIAL PRESSURE CELL
PRESSURE RELIEF VALVE

Fig. 4

reaction is endothermic, the reactor was jacketed and the temperature of the influent and effluent streams was held constant. Presented in Fig. 5 is a typical breakthrough curve and pressure drop plot. For this particular run, the pressure drop increase was noticeable and was not solely a function of bed conversion.

In the course of these fixed-bed studies, it was observed that for a given mass throughput, certain process conditions resulted in a greater pressure drop than others. In several instances, the increase in pressure drop during a run behaved in an autocatalytic manner and necessitated discontinuation of the run. The increase in pressure drop appeared to result from two phenomenom; a slow gradual increase that was a function of bed conversion and a rapid increase which was a function of relative humidity. The magnitude of the latter often overshadowed the former. The observed pressure drop plotted as a function of relative humidity at two temperatures, 295 and 305 K, and a superficial velocity of ~13 cm/s is presented in Fig. 6. It is significant that the data is consistent at the two temperatures as the saturation vapor pressures differed by a factor of 1.8. Furthermore, the dependency upon relative humidity indicates the presence of a surface adsorption phenomenon. For physical adsorption on surfaces, the extent of adsorption is dependent upon the extent of saturation, P/P_o, or in the case of water, the relative humidity. The fact that the pressure drop becomes more severe at ~60% relative humidity indicates that capillary condensation is likely present. As no hysteresis was observed during nitrogen adsorption studies, it is speculated that the condensation occurs at V-shaped contact points or pores. The presence of the condensed water then provides sites of rapid recrystallizaton. As the flaked reactant was prepared by the rapid cooling of a magma which was substoichiometric in octahydrate (7.0 to 7.9 waters of hydration), the rate of recrystallization is likely enhanced by a need to reduce internal energy locked up within the flake. This energy may be present as defects within the crystallites or surface energy resulting from the small size of the crystallities and the presence of the $Ba(OH)_2 \cdot 3H_2O$ -- $Ba(OH)_2 \cdot 8H_2O$ eutectic. Photographs of <u>commercial</u> $Ba(OH)_2 \cdot 8H_2O$ flakes after recrystallization at a

ORNL DWG 81-15756

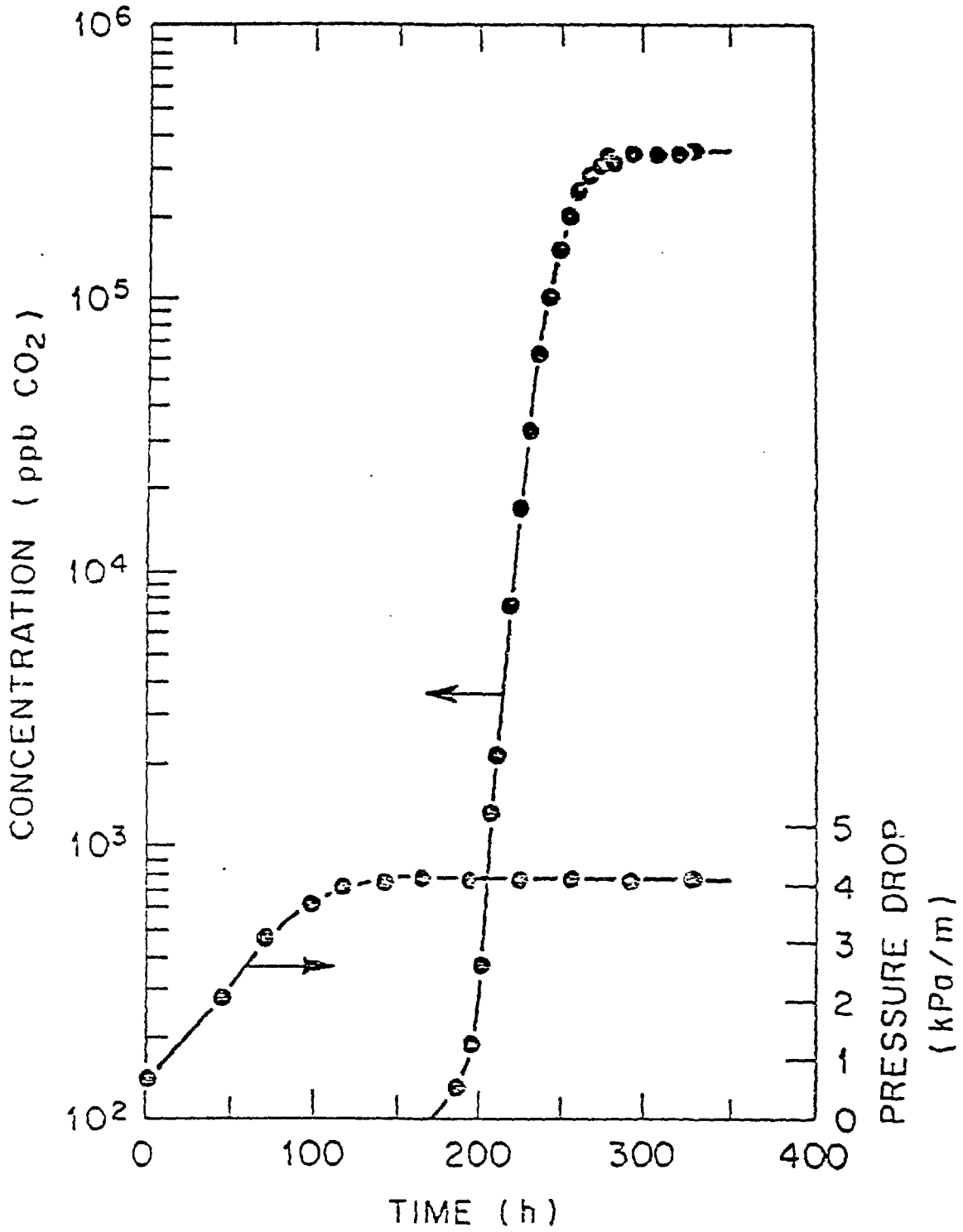

Fig. 5

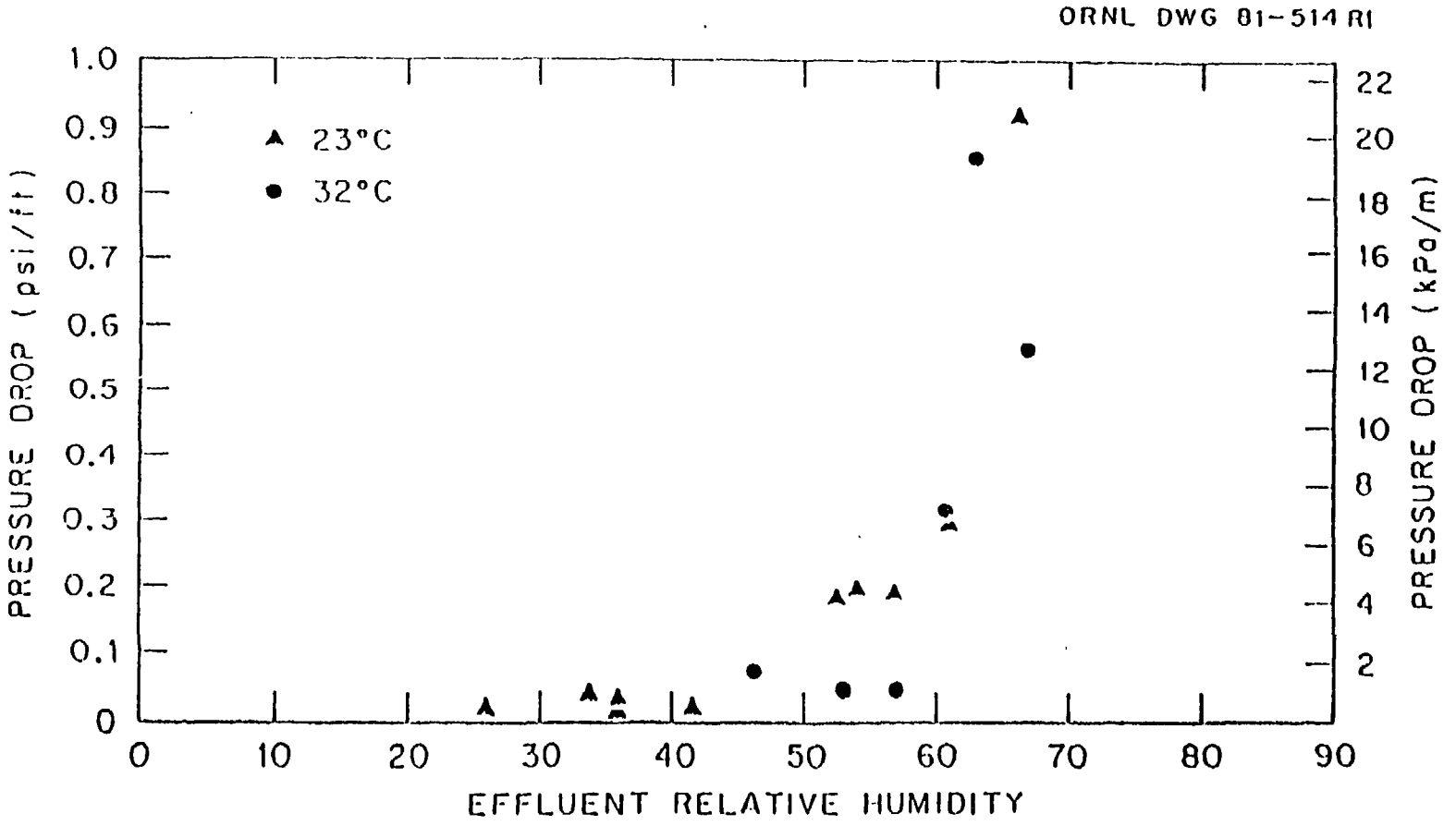

PRESSURE DROP AS A f(HUMIDITY) FOR THE $Ba(OH)_2 \cdot 8H_2O$ FIXED BEDS

Fig. 6

relative humidity in excess of 60% are presented in Fig. 7. For rehydration at lower humidities, external changes of the flake were small.

The functional dependency of pressure drop upon relative humidity is helpful in understanding the autocatalytic pressure drop behavior observed at high relative humidities. For a fixed influent water vapor concentration, any increase in system pressure at constant temperature will result in an increase in the water vapor pressure and likewise the relative humidity, P/P_o. Therefore as the pressure drop across the bed increases, so does the relative humidity within the bed and each continues to increase until the run must be terminated. At lower relative humidities, the rate of increase in pressure drop as a function of relative humidity is not sufficient to autocatalyze the process.

The pressure drop dependency upon relative humidity also restricts the upper flowrate which the process may treat. Increased gas flows result in greater pressure drops across the bed (i.e. a greater pressure at the entrance to the bed). Therefore the relative humidity at the entrance of the bed must be <60%, but the influent water vapor pressure must be greater than the dissociation vapor pressure of $Ba(OH)_2 \cdot 8H_2O$.

Extensive modeling studies were performed on the breakthrough curves from the fixed-bed studies. Because of the nature of the governing partial differential equations and their respective boundary conditions, solutions were of a numerical nature. An in-depth review of the method of analysis and the associated assumptions is presented elsehwere.[32] The analysis indicated that the rate expression could be modelled by an equation of the form:

$$R = K_F A_o (1-X) C$$

where

K_F = gas film mass transfer coefficient,

A_o = initial surface area available for mass transfer,

X = fractional conversion of reactant, and

C = bulk CO_2 concentration.

Fig 11

Data analysis indicated K_FA_O to be a weak function of temperature and a strong function of velocity, indicative of gas-film control. Considerable dispersion in the value of the K_FA_O coefficients were observed for a given mass throughput. There were indications that the dispersion resulted from differences in the actual area available for mass transfer and the possible presence of localized channeling. Based upon published correlations for the K_F coefficient, the correlation for the K_FA_O coefficient possessed a greater functional dependency upon velocity than expected. Because the studies were conducted on flaked material with considerable interparticle contact, it is speculated that the amount of surface area available for mass transfer increased as a function of gas velocity, thus resulting in the greater than anticipated functional dependency of K_FA_O upon velocity. This factor may also account for the greater than anticipated dispersion in K_FA_O as some localized packing arrangements would be more conducive to restructuring. A representative breakthrough curve and the model-predicted curve are presented in Fig. 8.

V. Pilot Unit Development

In the development of this fixed-bed technology, a pilot unit capable of processing 34 m^3/h (20 ft^3/min) was designed, constructed, and is currently in operation. Specific goals of this aspect of process development are:

A. Provide the basis for the design of a ^{14}C immobilization module for future testing under hot conditions.

B. Provide data at operating conditions not achievable with present bench-scale equipment, in particular operation at near-adabatic conditions.

C. Provide necessary scale-up data.

D. Provide operating data on key hardware items and instrumentation.

Presented in Fig. 9 is a flow schematic of the ^{14}C Immobilization pilot unit. A photograph of the system is presented in Fig. 10. The designed gas throughput at a superficial velocity of 13 cm/s in the reactor is 34 m^3/h (20 ft^3/min). The system

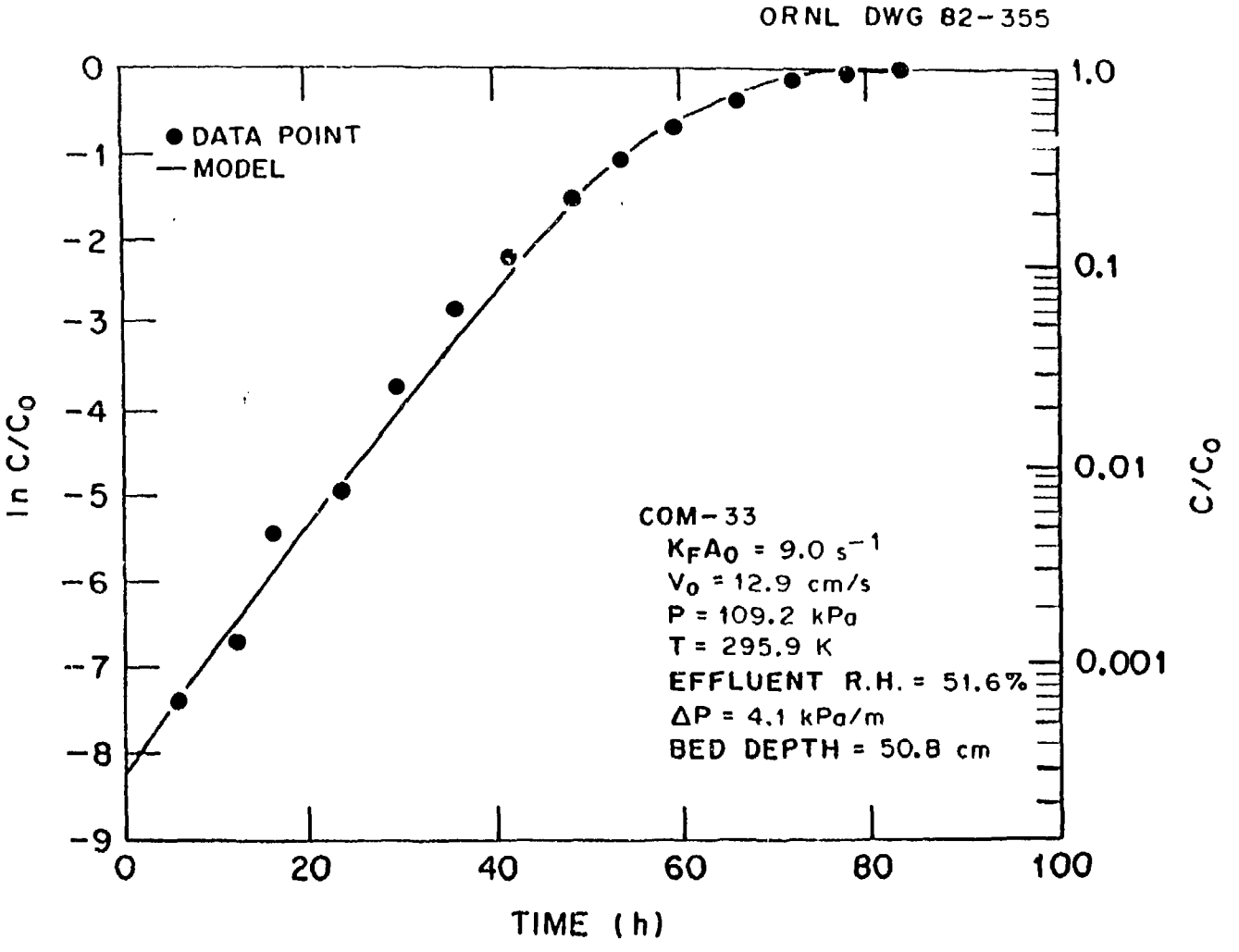
ORNL DWG 82-355
DATA POINT
MODEL
COM-33
$K_F A_0$ = 9.0 s^{-1}
V_0 = 12.9 cm/s
P = 109.2 kPa
T = 295.9 K
EFFLUENT R.H. = 51.6%
ΔP = 4.1 kPa/m
BED DEPTH = 50.8 cm
ln C/C0
C/C0
TIME (h)
0
-1
-2
-3
-4
-5
-6
-7
-8
-9
1.0
0.1
0.01
0.001
0
20
40
60
80
100

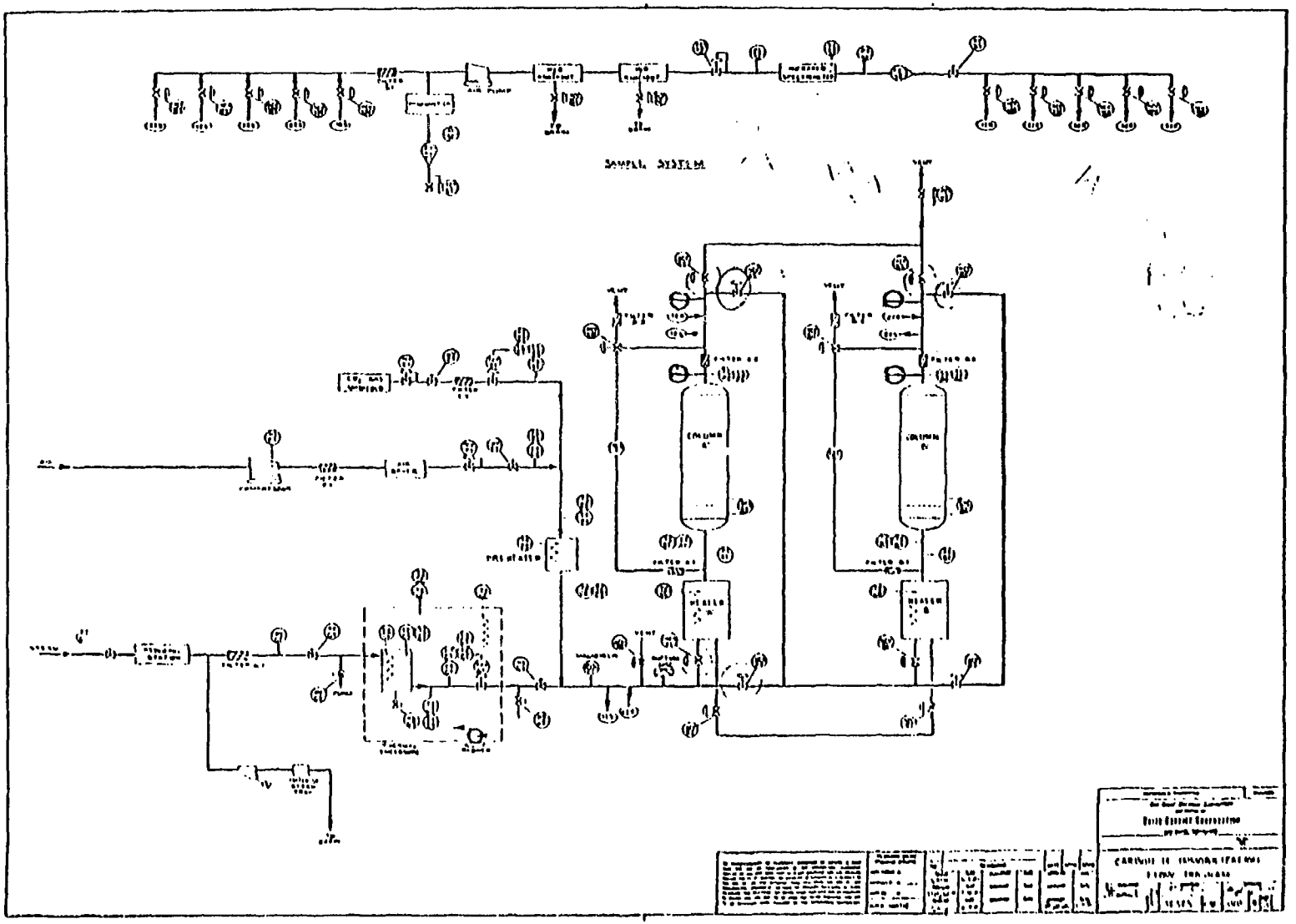

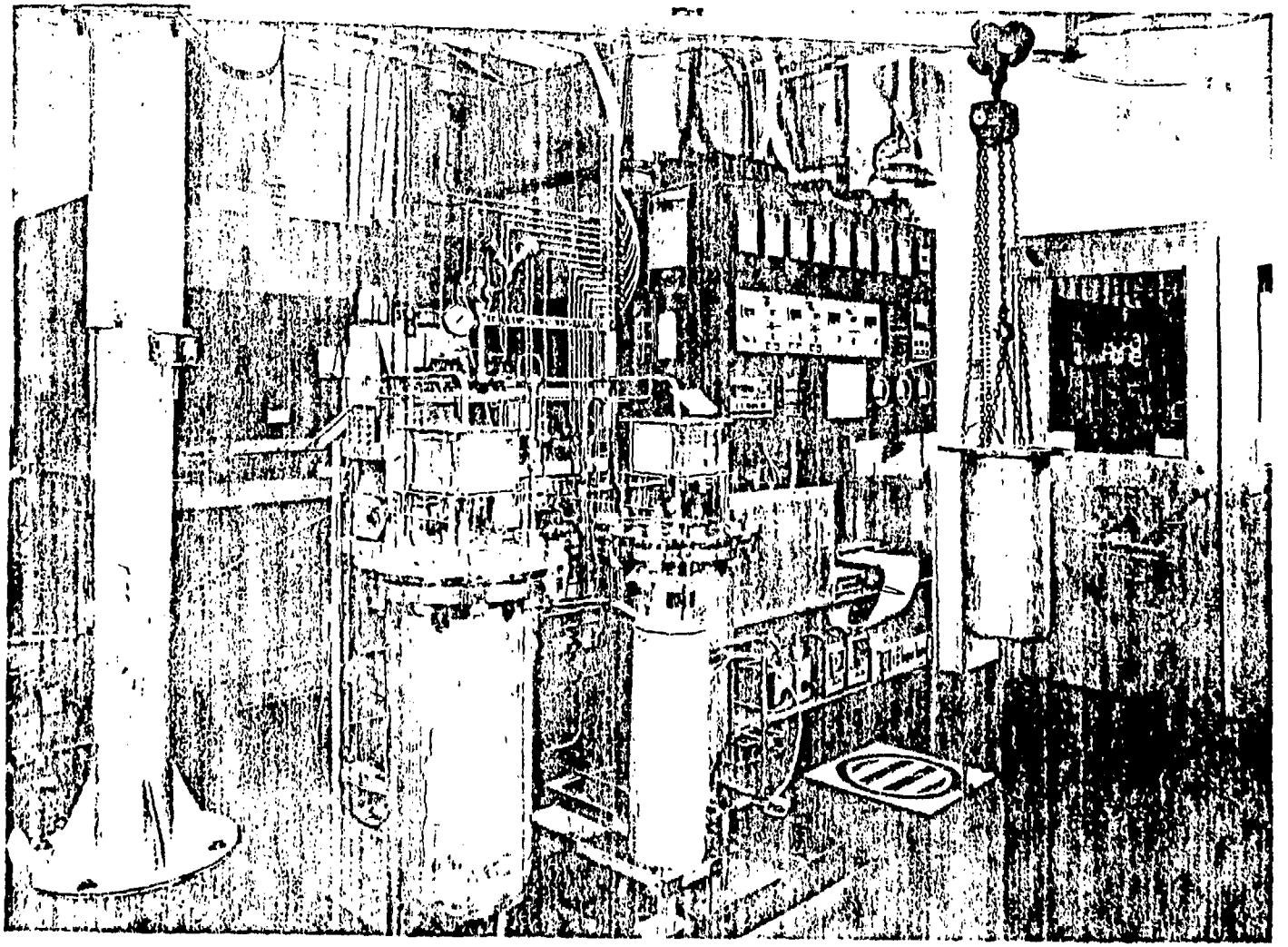

consists of 2 reactors which contain cannisters loaded with 32 kg (70 lb) of commercial $Ba(OH)_2 \cdot 8H_2O$ reactant. Due to the size of the cannisters and the relatively long loading times prior to breakthrough, continuous operation with only two reactors is possible. The steam, air, and CO_2 flow stations are unique to our pilot unit and will not be discussed in detail.

The overall pilot unit is controlled by a 5TI Logic Controller manufactured by Texas Instruments. The unit is presently capable of monitoring 8 DC and 16 AC input signals and providing 24 DC and 16 AC output signals. The logic controller monitors alarm signals from the CO_2 analyzer, the hygrometer, flowmeters, timers, and pressure and temperature sensors. Upon sensing an alarm condition such as a CO_2 concentration of 1 ppm_v in the effluent gas stream, valves are actuated in the proper sequence at prescribed time intervals thus diverting flow to the second column. Numerous 3/4 and 1/4-in. Whitey ball valves are located within the system for bulk flow control and for gas sampling. For valve actuation, electronic DC signals from the logic controller are converted to pneumatic signals using modular Humphrey TAC electric air valves. The Whitey ball valves are then actuated pneumatically via Whitey actuators. Gas samples may be routinely taken and returned from any one of 5 points within the system. Sampling from these locations may be controlled by the logic controller. The sample gas is filtered and a portion of it fed to a General Eastern Model 1200 APS hygrometer sensor. The unit utilizes the "vapor condensation on a mirror" principal thus providing a true dewpoint determination. Because of the small sensor volume and the resulting small gas throughput (.5 L/min), this portion of the gas sample is vented to the atmosphere. The remainder of the sample gas is pressurized via a metal bellows pump, fed to 2 knockout vessels for H_2O removal, and to a Wilks-Foxboro Miran 1A infrared spectrometer. This unit is capable of analyzing CO_2 over the continuous 100 ppb_v to 330 ppm_v C_2 range and has been described elsewhere.[21,32] Because of the 5.6 L sensor volume and to insure an adequate instrument response time, the gas throughput is appreciable and the sample stream is recycled to the pilot unit.

Gas preheaters connected to Barber-Coleman Series 520 temperature controllers are located before each reactor to provide the desired influent temperature. The pressure drop across each column and the gauge pressure at the base of the column are monitored via Foxboro Model E13DH differential pressure cells. Dwyer Photohelix pressure gauges/switches monitor the pressure drop across the gas distributors and HEPA filters. Thermocouples are located throughout the system for temperature control and sensing. Original plans were to enclose the pilot unit in a thermal-regulated structure, thus enabling studies at 30 and 40°C under highly controlled conditions to be conducted. These studies are currently in jeopardy because of funding uncertainties.

Whereas prior studies on the 10.2-cm-I.D. fixed beds were conducted at near-isothermal conditions, the pilot unit studies are being conducted under near-adiabatic conditions. For the treatment of an air-based (330-ppm_V-CO_2) gas stream, one would predict a temperature drop of ~4°C in the gas stream due to the endothermic nature of the reaction (364 kJ/mol). Such a temperature drop has been experimentally verified. Because of the sensitivity of the operational characteristics of the bed (i.e. pressure drop) upon relative humidity and the dependancy of relative humidity upon system temperature, the results from these studies are extremely valuable in determining conditions for optimal process operation. Studies will also be conducted to determine if preconditioning of the bed prior to contact with CO_2 is beneficial in reducing pressure drop problems. During the preconditioning step, the substoiciometric commercial $Ba(OH)_2 \cdot 8H_2O$ will be hydrated to $Ba(OH)_2 \cdot 8H_2O$ at conditions which ensure the retention of flake integrity (a relative humidity <60%). It is speculated that pressure drop problems during subsequent CO_2 removal at relative humidities >60% will be reduced.

VI. Conclusion

Extensive studies have been conducted upon $Ba(OH)_2$ hydrates, their reaction with CO_2, and the operation of a fixed-bed process for CO_2 removal. Micro-scale

studies indicated (1) the published vapor pressure data for $Ba(OH)_2 \cdot 8H_2O$ to be valid, (2) the rate of dehydration or rehydration to be proportional to the amount of free water on the surface (i.e. a function of relative humidity), and (3) the reactivity of $Ba(OH)_2 \cdot 8H_2O$ for CO_2 to be 3 orders of magnitude greater than that of either $Ba(OH)_2 \cdot 3H_2O$ or $Ba(OH)_2 \cdot H_2O$. Macro-scale studies under near-isothermal conditions on 10.2-cm-ID fixed beds of commercial $Ba(OH)_2 \cdot 8H_2O$ flakes indicated that the pressure drop across the bed increased dramatically as 60% relative humidity in the effluent gas was approached. It is speculated that this phenomenom results from the capillary condensation of water at V-shaped contact points or pores and that this facilitates the subsequent rehydration and recrystallization of the flake. Although the resulting flakes have greater external surface area, they are more fragile and degrade more readily upon conversion to $BaCO_3$, thus resulting in increased pressure drop across the fixed beds.

Experimental studies indicated the transfer of the reactant gas through the gas film to be the major resistance to mass transfer. A model, assuming gas film control, was developed and exact numerical solutions obtained. An excellent correlation between the model-predicted breakthrough curves and the experimental breakthrough curve was obtained when the area available for mass transfer was modeled as a linear function of conversion [i.e. $A=A_o(1-X)$]. The magnitude of the mass transfer coefficient was characteristic of literature values. There were indications that the magnitude of the initial surface area available for reaction, A_o, may be a weak function of velocity due to a reallignment of the flakes. This reallignment results from fluid shear forces and an accompanying reduction in the number of planar contact points between neighboring flakes, thus increasing the area available for mass transfer.

Based upon the experimental data obtained during this study and its subsequent analyses, a window or regime of optimal process operation under near-isothermal conditions was determined to exist for the fixed-bed process. The window is bounded on the lower side by the dissociation vapor pressure of $Ba(OH)_2 \cdot 8H_2O$ and on the

ORNL DWG 82-306

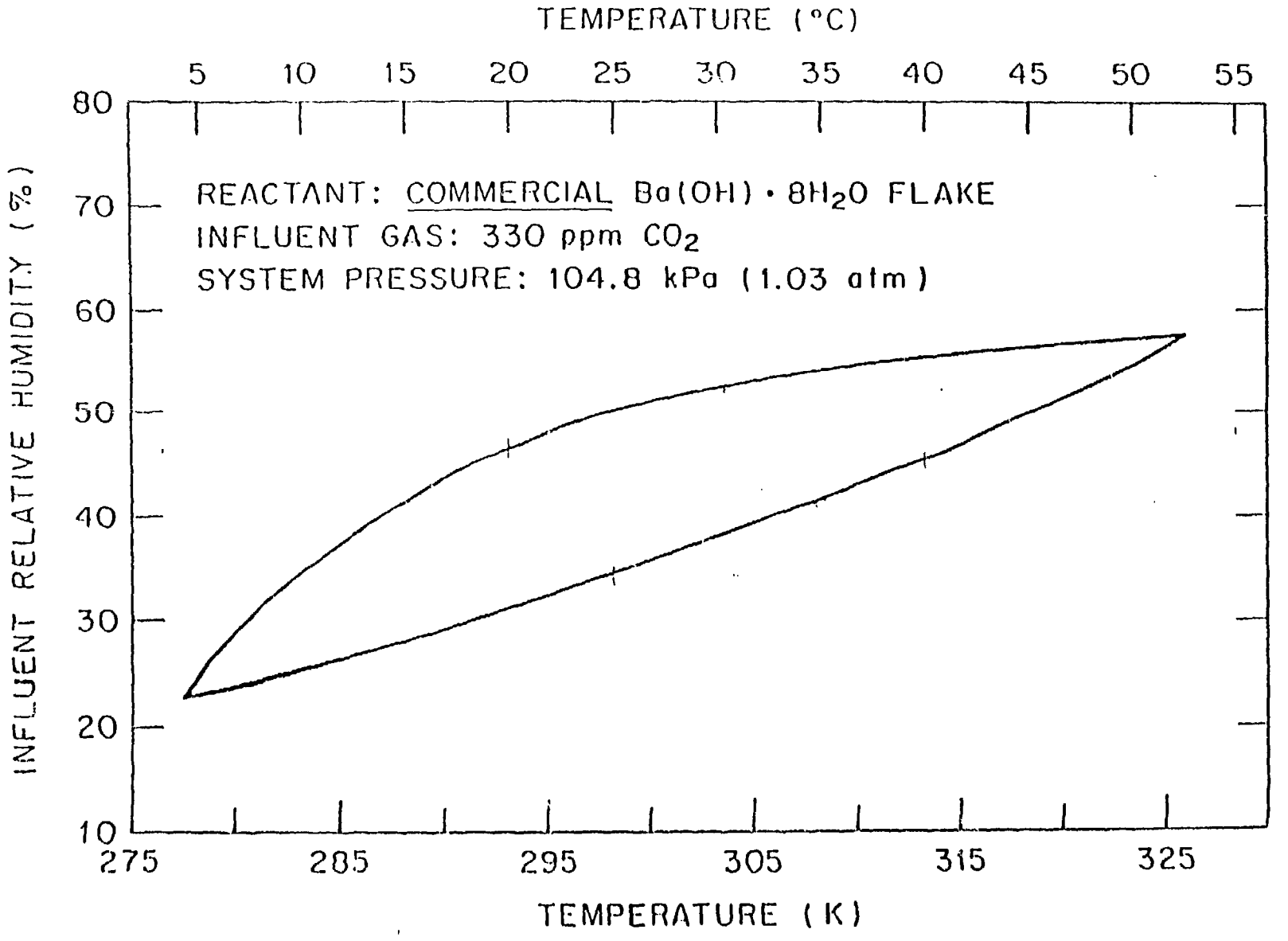

upper side by the onset of appreciable capillary condensation and subsequent pressure drop problems (~60% relative humidity). An operating envelope is presented in Fig. 11 for the treatment of 330 ppm_V CO_2 gas stream at a system pressure of 104.8 kPa (.5 psig). The relative humidity of the influent gas must fall within the envelope for optimal gas throughput. If changes are made in either the CO_2 concentration, thus affecting the amount of water vapor produced, or the system pressure, which will affect the partial pressure of the water vapor and subsequently the relative humidity (P/P_o), the operating envelope will change. The operating envelope also demonstrates why operational problems at 22 and 32°C were not severe and considerable difficulty was encountered when trying to operate the process at 42°C.

Successful isothermal operation of the process at higher effluent relative humidities (>60%) is possible by significantly reducing the gas throughput. The effect of operating the bed at conditions of water vapor saturation, whereby the water product would remain in the bed and the reaction would become exothermic, was not examined in detail. However, the reaction does proceed readily at these conditions and the $BaCO_3$ product is extremely insoluble.

Studies are underway on a pilot unit to determine the effects of operation at near-adiabatic conditions, whereupon the endothermic reaction results in a 4°C drop in the gas temperature upon passing through the bed. The authors speculate that complete reactant utilization and an acceptable pressure is possible when the relative humidity, based upon the influent water vapor pressure and the effluent saturation vapor pressure, falls within the operating window. This speculation is based upon a relative comparison of the rate of axial movement of the reaction zone through the bed and the rate of dehydration and accompanying deactivation of commercial $Ba(OH)_2 \cdot 8H_2O$ flakes. Furthermore, studies are underway to determine if prior hydration of the water-deficient commercial $Ba(OH)_2 \cdot 8H_2O$ to $Ba(OH)_2 \cdot 8H_2O$ at conditions which retain the integrity of the flake, a relative humidity <60% and a water vapor pressure > the dissociation vapor pressure of $Ba(OH)_2 \cdot 8H_2O$, will enable

subsequent CO_2 removal at much higher relative humidites in the absence of significant pressure drop problems.

References

1. H. Bonka et al., "Contamination of the Environment by Carbon-14 Produced in High-Temperature Reactors," *Kernetechnik 15*(7), 297 (1973).

2. W. Davis, Jr., *Carbon-14 Production in Nuclear Reactors,* ORNL/NUREG/TM-12 (February 1977).

3. C. D. Kunz, "Continuous Stack Sampling for ^{14}C at the R. E. Ginna Pressurized Water Reactor," *Trans. Am. Nucl Soc.* 38,100 (1981).

4. C. O. Kunz, W. E. Mahoney, and T. W. Miller, "Carbon-14 Gaseous Effluents from Boiling Water Reactors," *Trans. Am. Nucl. Soc. 21,* 91 (1975).

5. C. O. Kunz, W. E. Mahoney, and T. W. Miller, "C-14 Gaseous Effluent from Pressurized Water Reactors," pp. 229-234 in *Proceedings of the Health Physics Society 8th Midyear Symposium,* Knoxville, Tenn., 1974, CONF 741018.

6. M. J. Kabat, "Monitoring and Removal of Gaseous Carbon-14 Species," Proceedings of the *15th DOE Nuclear Air Cleaning Conference,* Boston, Mass., Aug. 7-10, 1978.

7. H. Schuttelkopf, *Releases of $^{14}CO_2$ from Nuclear Facilities with Gaseous Effluents,* Kernsforschungszentrum Karlsruhe KFK 2421, June, 1977 (translated from German) ORNL-tr-4527.

8. *Program Strategy Document for the Management of Radioactive Airborne Wastes - Draft,* Exxon Nuclear Idaho Company, Inc., prepared for Dept. of Energy, Idaho Operations Office (Dec 1981).

9. P. J. Magno, C. B. Nelson, and W. H. Ellett, "A Consideration of the Significance of Carbon-14 Discharges from the Nuclear Power Industry," p. 1047 in *Proceedings of the Thirteenth AEC Air Cleaning Conference,* San Francisco, Calif., Aug. 12-15, 1974, CONF-740807.

10. G. G. Killough, *A Diffusion-Type Model of the Global Carbon Cycle for the Estimation of Dose to the World Population from Releases of Carbon-14 to the Atmosphere,* ORNL/TM-5269 (1977).

11. G. G. Killough et al., *Progress Report on Evaluation of Potential Impact of ^{14}C Releases from an HTGR Reprocessing Facility,* ORNL/TM-5284 (July 1976).

12. L. Machta, "Prediction of CO_2 in the Atmosphere," *Carbon and the Biosphere,* G. M. Woodwell and E. V. Pecan, eds., Technical Information Center, Office of Information Services, U.S. Atomic Energy Commission (August 1973).

13. J. W. Snider and S. V. Kaye, "Process Behavior and Environmental Assessment of ^{14}C Releases from an HTGR Fuel Reprocessing Facility," *Proceedings of the ANS-AIChE Topical Meeting,* Sun Valley, Idaho, Aug. 5-6, 1976.

14. L. Pauling, "Genetic and Somatic Effects of Carbon-14," *Science 128*, 1183 (1958).

15. J. Schwibach, H. Riedel, and J. Bretschneider, *Studies on the Emission of Carbon-14 from Nuclear Facilities (Nuclear Power Plants and Reprocessing Plants): Its Measurement and the Radiation Exposure Resulting from Emissions*, Series of the Institute for Radiation Hygiene of the Federal Health Office, No. 20, 1979 (translated from German) OLS-80-233.

16. *Radiological Significance and Mangement of Tritium, Carbon-14, Krypton-85, Iodine-129 Arising from the Nuclear Fuel Cycle*, Nuclear Energy Agency, Organization for Economic Cooperation and Development, Paris, France 1980.

17. G. C. Killough and P. S. Rohwer, "A New Look at The Dosimetry of ^{14}C Released to The Atompshere as Carbon Dioxide," *Health Physics*, 4,141 (1978).

18. G. C. Killough, J. E. Till, E. L. Etnier, B. D. Murphy, and R. J. Roridon, "Chapter 11, Dose Equivalent Due to Atmospheric Releases of Carbon," taken from *Models and Parameters for Environmental Radiological Assessment*, C. W. Miller Editor, DOE/TIC-11368 (in press).

19. G. C. Killough and J. E. Till, "Scenarios of ^{14}C Releases from The World Nuclear Industry from 1975 to 2020 and the Estimated Radiological Impact," *Nuclear Safety* 19(5):602 (1978).

20. T. W. Fowler and C. B. Nelson, *Health Impact Assessment of Carbon-14 Emmissions from Normal Operations of Uranum Fuel Cycle Facilities*, EPA 520/5-80-004 (1981).

21. G. L. Haag, "Carbon-14 Immobilization via the CO_2–$Ba(OH)_2$ Hydrate Gas-Solid Reaction," *Proceedings of the 16th DOE Nuclear Air Cleaning Conference*, San Diego, CA, Oct. 20-23, 1980.

22. *Handbook of Chemistry and Physics*, 52nd ed., The Chemical Rubber Co., Cleveland, Ohio, 1972, pp. 13-70.

23. W. F. Linke and A. Seidell, *Solubilities of Inorganic and Metal Organic Compounds*, Fourth ed., American Chemical Society, Washington, D.C., 1958.

24. A. G. Croff, *An Evaluation of Options Relative to the Fixation and Disposal of ^{14}C-Contaminated CO_2 as $CaCO_3$*, ORNL/TM-5171 (April 1976).

25. A. G. Evans, W. E. Prout, J. T. Buckner, and M. R. Buchner, Management of *Radioactive Waste Gases from the Nuclear Fuel Cycle - Volume 1, Comparison of Alternatives*, NUREG/CR-1546, DPST-NUREG-80-5, Vol. 1. (1980).

26. D. W. Holladay, *Experiments with a Lime Slurry in a Stirred Tank for the Fixation of Carbon-14 Contaminated CO_2 from Simulated HTGR Fuel Reprocessing Off-Gas*, ORNL/TM-5757 (1978).

27. D. W. Holladay, *An Experimental Investigation of the Distribution of Krypton from Simulated HTGR Fuel Reprocessing Off-Gas During the Removal and Fixation of CO_2 by the CO_2-$Ca(OH)_2$ Slurry Reaction, Reaction*, ORNL/TM-6539 (in preparation).

28. D. W. Holladay and G. L. Haag, "Removal of ^{14}C-Contaminated CO_2 from Simulated LWR Fuel Reprocessing Off-Gas by Utilizing the Reaction Between CO_2 and Alkaline Hydroxides in Either Slurry or Solid Form," pp. 548-569 in *Proceedings of the 15th DOE Nuclear Air Cleaning Conference*, Boston, Mass., Aug. 7-10, 1978.

29. K. J. Notz, D. W. Holladay, C. W. Forsberg, and G. L. Haag, "Processes for the Control of $^{14}CO_2$ During Reprocessing," paper presented at the International Symposium on Management of Gaseous Wastes from Nuclear Facilities, Vienna, Austria, Feb. 18-22, 1980.

30. G. R. Bray, C. L. Miller, T. D. Nguyen and J. W. Rieke, *Assessment of Carbon-14 Control Technology and Costs for the LWR Fuel Cycle*, EPA 520/4-77-013 (1977).

31. J. L. Kovach, *Review of Carbon-14 Control Technology and Cost*, NUCON 8EP555/01 (1979).

32. G. L. Haag, *Application of the CO_2-$Ba(OH)_2 \cdot 8H_2O$ Gas-Solid Reaction for the Treatment of Dilute Co_2-Bearing Gas Streams*, Ph.D. Dissertation, University of Tennessee, Knoxville, TN (in preparation).

G. L. Haag, *Application of the CO_2-$Ba(OH)_2 \cdot 8H_2O$ Gas-Solid Reaction for the Treatment of Dilute CO_2-Bearing Gas Streams*, ORNL-5887 (in preparation).

33. G. L. Haag, G. C. Young, J. W. Nehls, Jr., *Pilot Unit Development of the CO_2-$Ba(OH)_2 \cdot 8H_2O$ Gas-Solid Reaction for ^{14}C Immobilization*, ORNL/TM-8433, (in preparation).

34. Jim Nillis, Sherwin Williams Company, Coffeeville, Kansas, personal communication, 1981.

35. M. Michaud, "Contribution to the Study of the Hydroxides of Potassium and Barium," *Revue de Chimie Minerale*, -.5, 89 (1968). Translated from French by ORNL Translation Department.

36. M. Michaud, "Inorganic Chemistry - Study of the Binary Water-Barium Hydroxide System," *C. r. hepd. Se'anc. Acad. Sci. Paris 262.CV, 1143 (1966).*

37. B. A. Kondakov, P. V. kovtunenko, and A. A. Bundel, "Equilibria Between Gaseous and Condensed Phases in the Barium Oxide - Water System," *Russ. J. Phys. Chem. 38(1), 99-102 (1964).*

Fig. 1. Photograph of commercial $Ba(OH)_2 \cdot 8H_2O$ flaked reactant and $BaCO_3$ flaked product. The product was obtained at a process relative humidity <60%.

Fig. 2. Scanning electron micrographs of a flake of commercial $Ba(OH)_2 \cdot 8H_2O$ (top) and the $BaCO_3$ product. The product was obtained at a process humidity <60%. (Original photo - 8.9 x 11.4 cm, magnification — 5000X).

Fig. 3. Photograph of the microbalance system.

Fig. 4. Schematic of the fixed-bed experimental equipment.

Fig. 5. Logarithm of the experimental breakthrough profile and the change in pressure drop across the bed presented as function of times, superficial gas velocity of ~13 cm/s.

Fig. 6. Pressure drop as a function of relative humidity during fixed-bed studies on commercial $Ba(OH)_2 \cdot 8H_2O$ flakes, superficial gas velocity of ~13 cm/s.

Fig. 7. Top and bottom views of a commercial $Ba(OH)_2 \cdot 8H_2O$ flake subjected to relative humidity >60%.

Fig. 8. Breakthrough curve and model-predicted breakthrough curve for a typical fixed-bed run.

Fig. 9. Schematic of the ^{14}C Immobilization pilot unit.

Fig. 10. Photograph of the ^{14}C Immobilization pilot unit.

Fig. 11. Operating window for the contacting of a 330 ppm_v CO_2 gas stream with fixed beds of commercial $Ba(OH)_2 \cdot 8H_2O$ flakes under isothermal conditions.